Desalination and Water Treatment
www.deswater.com

doi: 10.1080/19443994.2016.1138895

57 (2016) 24467–24475
November

Taylor & Francis
Taylor & Francis Group

Preparation and adsorption properties of magnetic mesoporous Fe_3C/carbon aerogel for arsenic removal from water

Guozhu Shen[a], Yewen Xu[b,*], Bin Liu[a]

[a]*School of Physics and Optoelectronic Engineering, Nanjing University of Information Science & Technology, Nanjing 210044, China, Tel. +86 25 58731031; emails: shengz@nuist.edu.cn (G. Shen), liubinseu@163.com (B. Liu)*
[b]*Science and Technology on Near-Surface Detection Laboratory, Wuxi 214035, China, Tel./Fax: +86 510 68757022; email: yewen_xu@126.com*

Received 12 September 2015; Accepted 1 January 2016

ABSTRACT

Carbon materials are effective for removal of both toxic inorganic and organic substances. In this study, a novel magnetic mesoporous carbon aerogel which combined high specific surface area, adsorption capacity and magnetic property of Fe_3C was prepared by citrate sol-gel method. The as-prepared samples were characterized by powder X-ray diffraction, TEM, scanning electron microscope, and BET methods. Results show that the aerogel has the specific surface and average pore size of 290 m^2/g and 2.7 nm, respectively. Magnetic Fe_3C nanoparticles were dispersed uniformly in carbon matrix and exhibit excellent response to an external magnetic field. As a result, the adsorbent can be easily separated from solution using an external magnetic field. Batch experimental results on As(V) removal showed that the adsorption kinetics and isotherm data were fitted well by a pseudo-second-order model and a Freundlich model, respectively. The monolayer adsorption capacity (q_m) of the adsorbent was calculated to be 56.2 mg/g at pH 7.0. The excellent uptake capability of the magnetic mesoporous materials make it be potentially attractive materials for removal of hazardous substances from water.

Keywords: Arsenic removal; Adsorption kinetics and isotherm; Adsorption capacity; Mesoporous magnetic Fe_3C/Carbon aerogel

1. Introduction

The pollution of arsenic and its compounds is becoming more and more severe with the development of industry and economy. Arsenic mainly reaches humans through water supplies where it is generally present as As(III) and As(V) in the form of arsenite and arsenate. The inorganic arsenic is very poisonous for human beings. As a result, arsenic removal technologies, such as precipitation, coagulation, ion exchange, membrane filtration, foam floatation, solvent extraction, bioremediation, and adsorption, have attracted significant attention [1–4]. Among these technologies, adsorption is an inexpensive and commercially available technology. Many natural materials and specially designed technical particles including natural zeolite, clays, volcanic stone, modified activated carbon, metal and its oxides, and hydroxides such as iron, iron oxide, and cupric oxide [5–12], have been developed to remove arsenic from water. Furthermore, iron carbide is also a candidate

*Corresponding author.

for arsenic removal. Gutierrez-Muniz et al. reported that the iron carbide has a better adsorption capacity for As compared with Fe(0) and Fe_2O_3 [13].

However, the development of an adsorbent with a high surface area is necessary to increase the adsorption capacity of the material. Compared with bulk or commercial materials, nanomaterials are better candidates for adsorbents due to their high surface areas. However, nanopowder adsorbent easily aggregates, thus, this will result in the decrease of the nanomaterials surface area and adsorption sites, and the separation of powder nanomaterials from solution needs additional steps such as centrifugation, granulation by binder, and so on [14]. These will result in not only additional cost but also more complex operation. Therefore, different methods have been studied in order to increase specific surface area of adsorbent materials such as preparation of nanotubes [15–17], nanopores [18,19], films [20], impregnated nanoparticles [21,22], and chemical modification of adsorbents [23,24].

In this study, a simple sol-gel method was used to prepare magnetic porous adsorbents which combined high specific surface and magnetic property. The prepared materials were characterized by different technologies, and batch adsorption experiments were conducted for As(V) removal using the adsorbents. The objective of this study is to assess the adsorption capacity of the mesoporous adsorbent to As(V) and to effectively separate the adsorbent from aqueous solutions using external magnetic fields.

2. Materials and methods

2.1. Materials

All chemicals are of analytical grade and used without further purification, and all solutions were prepared with deionized water. Citric acid ($C_6H_8O_7{\cdot}H_2O$), ferric nitrate nonahydrate ($Fe(NO_3)_3{\cdot}9H_2O$), and ammonia were used for the adsorbent preparation. The As(V) stock solutions were prepared with sodium arsenate ($Na_3AsO_4{\cdot}12H_2O$). Sodium nitrate ($NaNO_3$) was used to fix a constant ionic strength (0.01 M $NaNO_3$) of solution. Sodium hydroxide (NaOH) and hydrochloric acid (HCl) were used to adjust the pH of solution.

2.2. Preparation of magnetic adsorbent

Magnetic adsorbents were prepared by citrate sol-gel method followed by annealing under nitrogen atmosphere. In a typical synthesis, 0.040 mol $C_6H_8O_7{\cdot}H_2O$ and 0.027 mol $Fe(NO_3)_3{\cdot}9H_2O$ ($C_6H_8O_7{\cdot}H_2O/Fe(NO_3)_3{\cdot}9H_2O$ molar ratio was 3:2) were dissolved in 40 ml deionized water, and pH of the above solution was adjusted to 7.0 using ammonia. The solution was evaporated at 80℃ for 2 h and then dried in air at 120℃ for 5 h to produce dry gel. The obtained gel was then annealed in N_2 at 800℃ for 1 h with a temperature ramp rate of 5℃/min. The prepared sample was denoted as S1. Other two samples S2 and S3 were prepared by adjusting the molar ratio of $C_6H_8O_7{\cdot}H_2O/Fe(NO_3)_3{\cdot}9H_2O$ to 2:1 and 3:1, respectively. Other procedures were the same as the above that of sample S1. Fig. 1 shows the preparation process of magnetic mesoporous Fe_3C/C aerogel.

2.3. Adsorbent characterization and analytical methods

The X-ray diffraction (XRD) patterns were collected on a Bruker D8 Diffractometer using Cu-Kα radiation (40 kV, 40 mA). Field emission scanning electron microscope (SEM) images were obtained on a JEOL JSM 7800 with accelerating voltages of 5.0 kV, while TEM images were taken on Philips Tecnai F20 (operated at 200 kV). Nitrogen adsorption isotherms were measured at 77 K using a TriStar II Surface Area and Porosity analyser. The samples were degassed under vacuum for 6 h at 180℃ before analysis. The specific surface areas (S_{BET}) were calculated using the Brunauer–Emmett–Teller (BET) method. The pore volumes and pore size distributions were derived from the adsorption branches of isotherms using the Barrett–Joyner–Halenda (BJH) model, whereas the total pore volumes (V_t) were estimated from the amount adsorbed at a relative pressure P/P_0 of 0.99. micropore volumes (V_{mi}) were determined according to the *t*-plot method. Arsenic concentration was determined by a Thermos Icap 6300 inductively coupled plasma–atomic emission spectroscopy (ICP-AES). Prior to analysis, the aqueous samples were diluted with deionized water to the testing range of the instrument.

2.4. Batch adsorption experiments

For all of three samples, batch tests were carried out at room temperature (25 ± 1℃) by adding 20 mg of prepared adsorbents into 150-mL glass vessels, containing 50 mL of 400 mg/L As(V) solution. The suspension was mixed with a mechanical orbit shaker. The pH of the solutions was adjusted with dilute HCl and NaOH solution to around 7.0 during shaking process. The suspensions were separated through an external magnetic field after they were shaken for 24 h; then, the equilibrium concentration was determined.

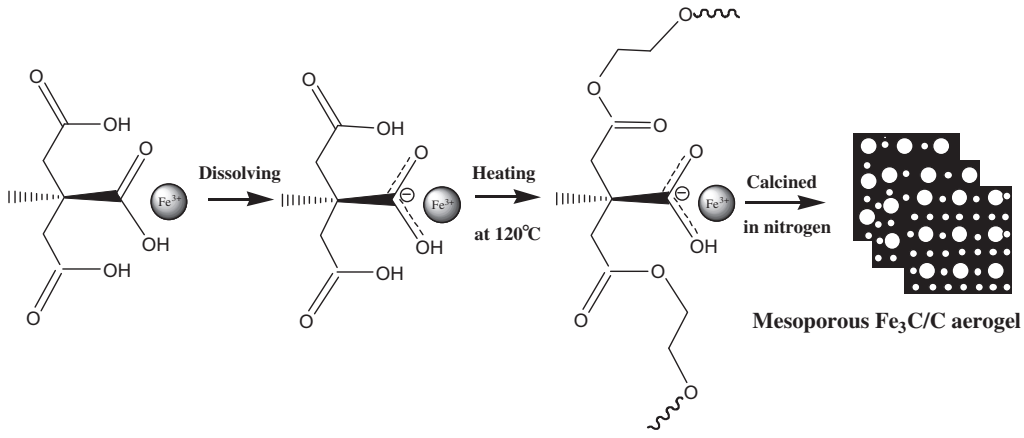

Fig. 1. The preparation process of magnetic mesoporous Fe_3C/C aerogel.

The kinetics experiments were carried out at room temperature (25 ± 1 ℃). A defined amount of arsenic stock solution was added in a 1,000mL glass vessel. Then, a corresponding amount of deionized water was added to make 500 mL of 5, 10 mg/L As(V) solution. The ionic strength was maintained at 0.01 M by adding 0.425 g sodium nitrate. After the solution pH was adjusted to 7.0 ± 0.3 by adding HCl or/and NaOH solution, 0.20 g of adsorbent was added to obtain a 0.40 g/L suspension. The suspension was mixed with a mechanical orbit shaker, and the pH was maintained at 7.0 ± 0.3 throughout the experiment. Approximately 5 ml aliquots were taken from the vessel at different time intervals and immediately separated. Then, the concentrations of arsenic in the separated solutions were determined.

The arsenic adsorption isotherm was determined using batch tests at the initial pH values of 7.0 ± 0.3. Initial arsenic concentration was varied from 5 to 40 mg/L. In each test, 20 mg of the adsorbent was loaded in the 150-mL glass vessel, and 50 ml of solution containing different amounts of arsenic was then added to the vessel. Ionic strength of the solution was adjusted to 0.01 M with $NaNO_3$. All samples were separated and analyzed for arsenic after the vessels were shaken for 24 h at 25 ± 1 ℃.

3. Results and discussion

3.1. Characterization of prepared adsorbents

Fig. 2(a) shows that the prepared sample exhibits excellent response to an external magnetic field. XRD pattern of the prepared adsorbents is illustrated in Fig. 2(b). It shows that the main diffraction peaks can be well indexed to orthorhombic Fe_3C (iron carbide) phase (JCPDS Card No. 35-0772) with a space group of *Pnma* for all samples. No peaks of any other crystal phases can be observed, confirming only Fe_3C crystal dispersed in carbon matrix.

The morphology of the synthesized products was examined by TEM and SEM. TEM images as shown in Fig. 3(a)–(c) demonstrate that the Fe_3C particles are aggregated with the size of 70–100 nm for the samples S1 and S2. However, the Fe_3C particles disperse uniformly in carbon matrix without any aggregation for sample S3, and the particle size is about 10 nm. The result shows that the higher the molar ratio of $C_6H_8O_7{\cdot}H_2O$ to $Fe(NO_3)_3{\cdot}9H_2O$, the narrower the distribution of nanoparticle size and more uniform particle size. Similarly, SEM images as shown in Fig. 3(d)–(f) show the same conclusion that smaller and smaller particle size can be found with increase in molar ratio of $C_6H_8O_7{\cdot}H_2O$ to $Fe(NO_3)_3{\cdot}9H_2O$. Fig. 3(g) shows the porous nature of cross section of the magnetic Fe_3C/C composites.

Nitrogen adsorption data confirm that the magnetic materials have characteristics that are typical for mesoporous materials: uniform pore-size distribution, high surface area, and large pore volume. This unique pore structure gives rise to a BET surface area of 113, 212, 290 m^2/g, a total pore volume of 0.10, 0.18, 0.22 cm^3/g, and a micropore volume of 0.01, 0.03, 0.06 cm^3/g, respectively, as shown in Fig. 4. Table 1 summarizes the textural characteristics of these materials. The total BET surface area and total volume exhibit an increasing tendency with the increase of molar ratio of $C_6H_8O_7{\cdot}H_2O$ to $Fe(NO_3)_3{\cdot}9H_2O$.

3.2. Adsorption kinetics

After 20 mg of each sample was added into 50 mL of arsenic solution and shaken for 24 h, the result

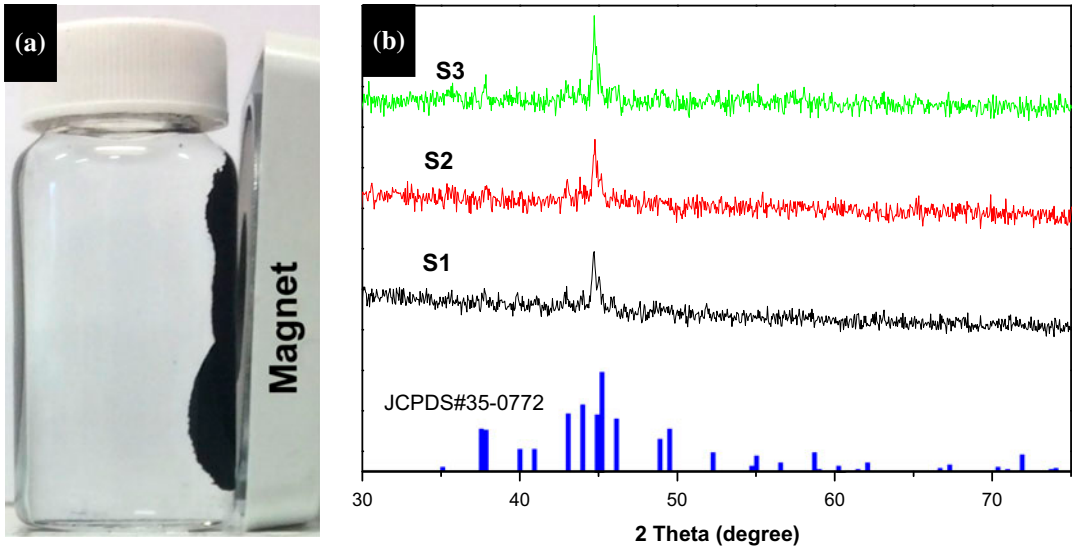

Fig. 2. Digital photograph (a) and the XRD pattern (b) of the prepared samples.

shows that the adsorption capacity is 42, 55, and 72 mg/g for samples S1, S2, and S3, respectively. According to the adsorption results along with the characterization of XRD, SEM, and BET, the sample S3 was selected to carry out adsorption kinetics and isotherm test.

Fig. 5(a) shows the variety of adsorption capacity with contact time. It is obvious that the adsorption process can be divided into two steps. In the first rapid step, over 80% of the equilibrium adsorption capacity was achieved within 3 h, and the contact time of 14 h was enough to achieve the adsorption equilibrium for both two initial concentrations. Fig. 5(b) shows the change in the arsenic concentration with time in aqueous phase.

In order to further investigate the mechanism of adsorption by the composite, the kinetics data of various initial concentrations were fitted to the pseudo-first-order and pseudo-second-order models, which were presented as follows in Eqs. (1) and (2), respectively [25,26]:

$$q_t = q_e(1 - e^{-k_1 t}) \quad (1)$$

$$\frac{t}{q_t} = \frac{t}{q_e} + \frac{1}{k_2 q_e^2} \quad (2)$$

where q_e and q_t are the adsorption capacities (mg/g) of the adsorbent at equilibrium and at any time t (h), respectively; and k_1 (h^{-1}) and k_2 (g/mg/h) are the related rate constants.

The rate constants obtained from pseudo-first-order and pseudo-second-order models are summarized in Table 2. The goodness of fit of the pseudo-second-order model to the experimental data was higher than the pseudo-first-order model as showed in Fig. 5(a) and checked from the calculated values of the correlation coefficient (R^2). This pseudo-second-order model assumes that the rate-limiting step may be chemisorption involving sharing or exchange of electrons between adsorbent and As(V), and that two reactions are occurring. The first one is fast and reaches equilibrium quickly and the second is a slower reaction that can continue for a long period of time. The rate constant k_2 of pseudo-second-order model decreases with increasing initial arsenic concentration, indicating that the adsorption may be more favorable at low solution concentration. The results are similar to those of metal oxides [8,27].

3.3. Adsorption isotherms

Adsorption isotherms were obtained at pH 7.0 ± 0.3 by varying the initial arsenic concentrations (5–40 mg/L). The isotherms obtained are presented in Fig. 6. Obviously, the slope of curve decreased gradually with the increase in initial arsenic concentration. That is to say, the adsorption percentage decreases with the increase in initial arsenic concentration. According to literature [28,29], adsorption of ions onto activated carbon occurs through parallel and consecutive reaction that involve the active sites on carbon surface and adsorbed ionic species. The

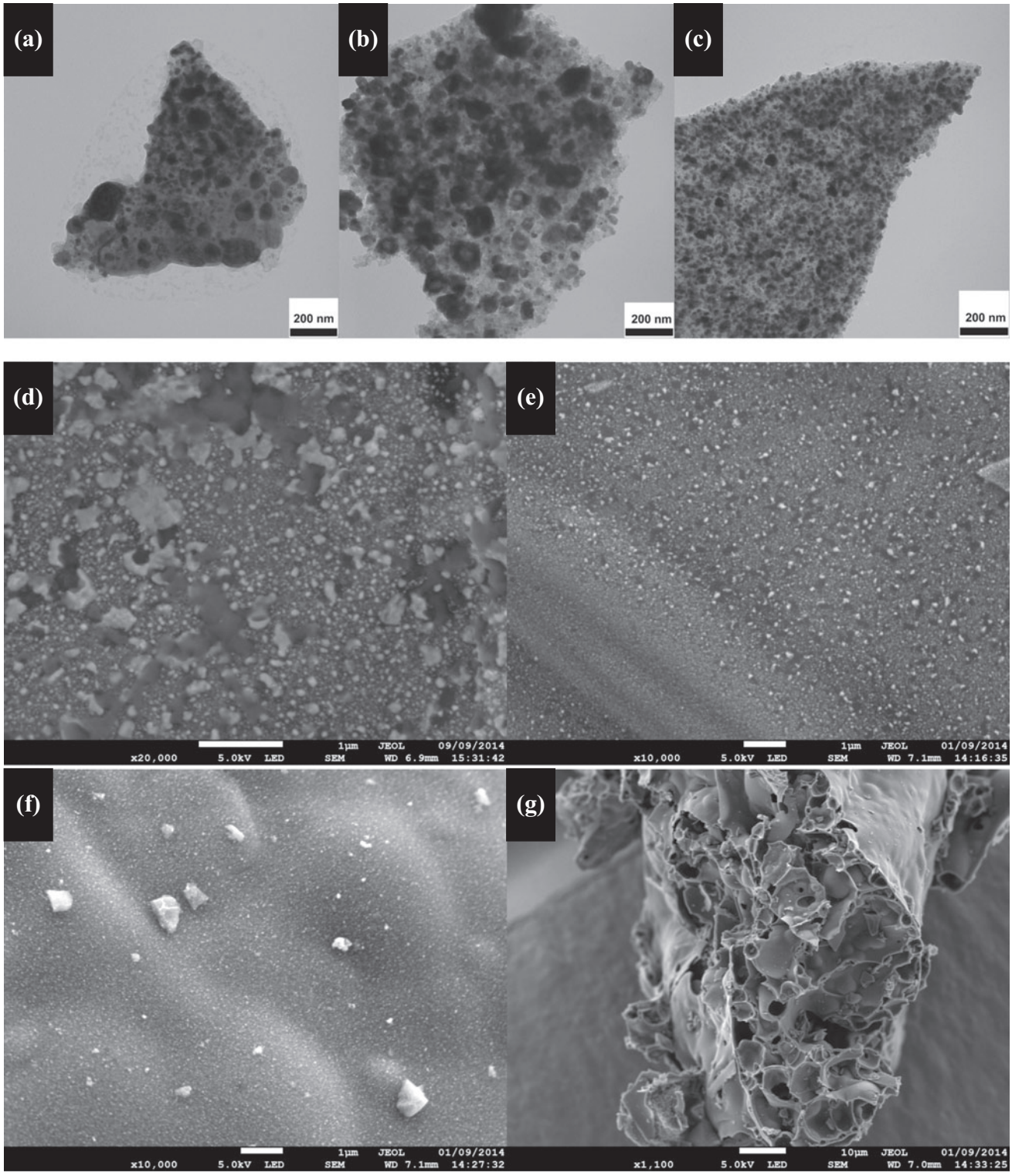

Fig. 3. TEM (a–c) and SEM (d–g) images of the samples S1 (a, d), S2 (b, e), and S3 (c, f, and g).

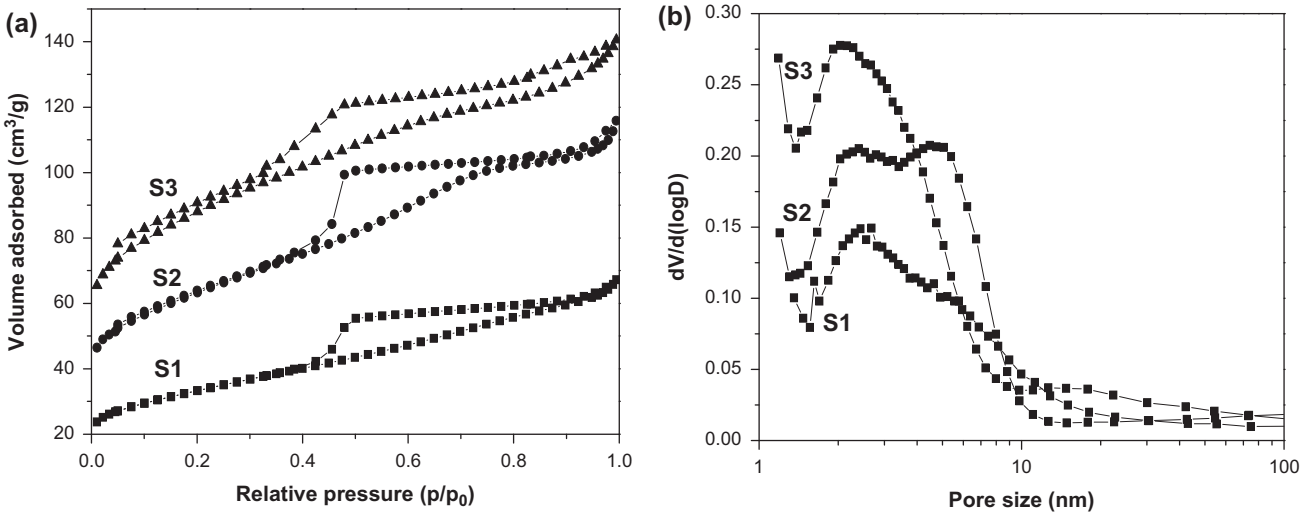

Fig. 4. Nitrogen adsorption isotherm (a) and pore size distribution (b) of the prepared samples.

Table 1
Textural parameters of the as-prepared magnetic aerogel materials (S_{BET}: BET surface area; V_t: total pore volume; V_{mi}: micropore volume; D_{me}: mesopore diameter)

Sample	S_{BET} (m^2/g)	V_t (cm^3/g)	V_{mi} (cm^3/g)	D_{me} (nm)
S1	113	0.10	0.01	3.5
S2	212	0.18	0.03	3.4
S3	290	0.22	0.06	2.7

dependence of equilibrium adsorption capacity on the process parameters is strictly correlated with their influence on concentration of ionic species in solution as well as on the adsorbent properties. The surface on carbon contains a large variety of ionizable groups which lead to the sorption of both anions and cations from aqueous phase. For the Fe_3C/carbon composite, an optimal pH value is around neutrality to maximize the adsorption capacity because the chemical species that play a role in the adsorption processes are $H_2AsO_4^-$ and $HAsO_4^{2-}$.

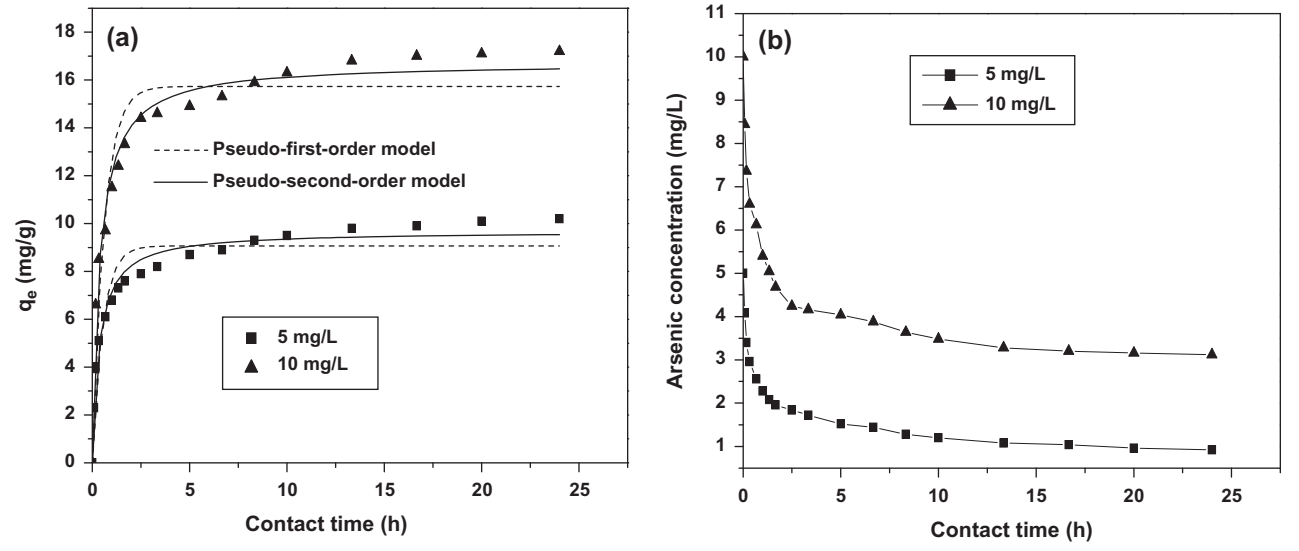

Fig. 5. (a) Kinetics of adsorption by magnetic composite. Symbols indicate experimental data; dash lines represent the pseudo-first-order model; solid lines refer to the pseudo-second-order model and (b) change in the concentrations of arsenic with time in the solution.

Table 2
Adsorption rate constant obtained from pseudo-first-order and pseudo-second-order models for different initial concentrations of As(V)

Initial concentration (mg/L)	Pseudo-first-order model			Pseudo-second-order model		
	k_1 (h^{-1})	q_e (mg/g)	R^2	k_2 (g/mg/h)	q_e (mg/g)	R^2
5	1.872	9.1	0.905	0.295	9.7	0.974
10	1.646	15.7	0.924	0.160	16.7	0.981

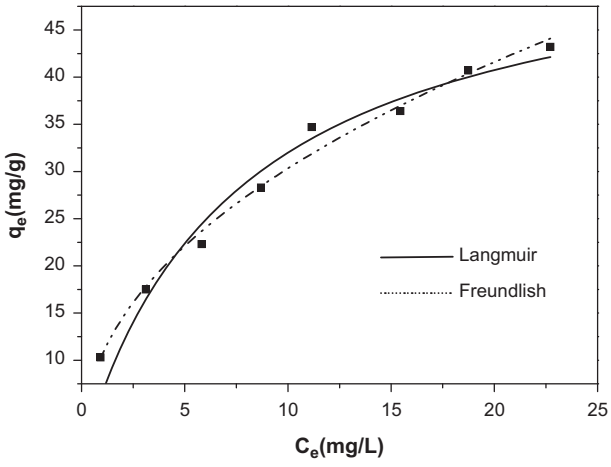

Fig. 6. Adsorption isotherms of arsenic. Symbols indicate experimental data; solid line represents the Langmuir model; dash line refers to the Freundlich model.

And the concentration of OH^- ion is sufficiently low to reduce the competition with the arsenic species [30]. In this case, the hydroxyl group in the FeOOH and COOH on the composite surface can easily exchange with the $H_2AsO_4^-$ and $HAsO_4^{2-}$ species in the aqueous solution [13,31,32]. To better understand the adsorption process, both Langmuir and Freundlich models were employed to describe the adsorption isotherms as shown in Fig. 6. The Freundlich equation is represented as:

$$q_e = K_F C_e^n \quad (3)$$

where q_e is the amount of arsenic adsorbed onto the solid phase (mg/g), C_e is the equilibrium arsenic concentration in the solution phase (mg/L), K_F is roughly an indicator of the adsorption capacity, and n is a constant related to the energy of adsorption in the model.

The Langmuir equation can be written in the form:

$$q_e = \frac{q_m b C_e}{1 + b C_e} \quad (4)$$

where q_e and C_e are as previously denoted, b is the equilibrium adsorption constant related to the affinity of binding sites (L/mg), and q_m is the maximum amount of the arsenic per unit weight of adsorbent for complete monolayer coverage.

Results of the calculated isotherms parameters as well as the goodness of the fit R^2 are shown in Table 3. It can be noted that equilibrium data fitted very well to both Langmuir and Freundlich models. Because the presence of magnetic Fe_3C particles in the adsorbent may lead to more heterogeneous surface, the Freundlich model which describes adsorption where the adsorbent has a heterogeneous surface with adsorption sites that have different energies of adsorption has higher goodness of fit as shown in Table 3. According to the Langmuir isotherm which represents the monolayer coverage adsorption model, the calculated adsorption capacity is 56.2 mg/g. This suggested that the magnetic mesoporous composite is effective for As(V) removal.

Table 3
Langmuir and Freundlich isotherm parameters for arsenic adsorption by the magnetic composite

As species	Langmuir model			Freundlich model		
	q_m (mg/g)	K_L (L/mg)	R^2	K_F (mg/g)	n (mg/g)	R^2
As(V)	56.2	0.132	0.967	10.6	0.456	0.988

4. Conclusion

In this study, citrate sol-gel method was used to prepare mesoporous Fe_3C/carbon aerogel precursor. The magnetic mesoporous Fe_3C/carbon aerogel materials were successfully obtained by a carbonization process at an annealing temperature of 800˚C under N_2 atmosphere. The BET results indicate that the specific surface area increases gradually with the increase in molar ratio of $C_6H_8O_7{\cdot}H_2O$ to Fe $(NO_3)_3{\cdot}9H_2O$. When the molar ratio was 3:1, the average pore size and the specific surface area of the mesoporous structures were 2.7 nm and 290 m^2/g, respectively. The magnetic mesoporous aerogel exhibited excellent response to an external magnetic field because of the magnetic nature of Fe_3C, resulting in easy separation of the magnetic mesoporous adsorbent from solution. The adsorption kinetics and isotherm data were fitted well by a pseudo-second-order model and a Freundlich model, respectively. The monolayer capacity (q_m) of the adsorbent for As(V) was calculated to be 56.2 mg/g. Therefore, the magnetic mesoporous Fe_3C/carbon aerogel has a significant potential in water treatment applications.

Acknowledgments

This work has been supported by Jiangsu Overseas Research & Training Program for University prominent young and middle-aged teachers and presidents and Science and Technology on Near-Surface Detection Laboratory.

References

[1] Z.L. He, S.L. Tian, P. Ning, Adsorption of arsenate and arsenite from aqueous solutions by cerium-loaded cation exchange resin, J. Rare Earths 30 (2012) 563–572.
[2] M. Sen, A. Manna, P. Pal, Removal of arsenic from contaminated groundwater by membrane-integrated hybrid treatment system, J. Membr. Sci. 354 (2010) 108–113.
[3] M.B. Baskan, A. Pala, A statistical experiment design approach for arsenic removal by coagulation process using aluminum sulfate, Desalination 254 (2010) 42–48.
[4] Q.Z. Feng, Z.Y. Zhang, Y. Chen, L.Y. Liu, Adsorption and desorption characteristics of arsenic on soils: Kinetics, equilibrium, and effect of $Fe(OH)_3$ colloid, H_2SiO_3 colloid and phosphate, Procedia Environ. Sci. 18 (2013) 26–36.
[5] C.A. Martinson, K.J. Reddy, Adsorption of arsenic(III) and arsenic(V) by cupric oxide nanoparticles, J. Colloid Interface Sci. 336 (2009) 406–411.
[6] M. Szlachta, V. Gerda, N. Chubar, Adsorption of arsenite and selenite using an inorganic ion exchanger based on Fe-Mn hydrous oxide, J. Colloid Interface Sci. 365 (2012) 213–221.
[7] A. Goswami, P.K. Raul, M.K. Purkait, Arsenic adsorption using copper (II) oxide nanoparticles, Chem. Eng. Res. Des. 90 (2012) 1387–1396.
[8] K. Wu, T. Liu, W. Xue, X.C. Wang, Arsenic(III) oxidation/adsorption behaviors on a new bimetal adsorbent of Mn-oxide-doped Al oxide, Chem. Eng. J. 192 (2012) 343–349.
[9] P.S. Kumar, L. Önnby, H. Kirsebom, Arsenite adsorption on cryogels embedded with iron-aluminium double hydrous oxides: Possible polishing step for smelting wastewater? J. Hazard. Mater. 250–251 (2013) 469–476.
[10] L. Yu, X.J. Peng, F. Ni, J. Li, D.S. Wang, Z.K. Luan, Arsenite removal from aqueous solutions by γ–Fe_2O_3-TiO_2 magnetic nanoparticles through simultaneous photocatalytic oxidation and adsorption, J. Hazard. Mater. 246–247 (2013) 10–17.
[11] X.H. Guan, T.Z. Su, J.M. Wang, Quantifying effects of pH and surface loading on arsenic adsorption on nanoactive alumina using a speciation-based model, J. Hazard. Mater. 166 (2009) 39–45.
[12] M. Asadullah, I. Jahan, M.B. Ahmed, P. Adawiyah, N.H. Malek, M.S. Rahman, Preparation of microporous activated carbon and its modification for arsenic removal from water, J. Ind. Eng. Chem. 20 (2014) 887–896.
[13] O.E. Gutierrez-Muñiz, G. García-Rosales, E. Ordoñez-Regil, M.T. Olguin, A. Cabral-Prieto, Synthesis, characterization and adsorptive properties of carbon with iron nanoparticles and iron carbide for the removal of As(V) from water, J. Environ. Manage. 114 (2013) 1–7.
[14] Y.F. Lin, J.L. Chen, Magnetic mesoporous Fe/carbon aerogel structures with enhanced arsenic removal efficiency, J. Colloid Interface Sci. 420 (2014) 74–79.
[15] H.Y. Niu, J.M. Wang, Y.L. Shi, Y.Q. Cai, F.C. Wei, Adsorption behavior of arsenic onto protonated titanate nanotubes prepared via hydrothermal method, Microporous Mesoporous Mater. 122 (2009) 28–35.
[16] S.A. Ntim, S. Mitra, Adsorption of arsenic on multiwall carbon nanotube-zirconia nanohybrid for potential drinking water purification, J. Colloid Interface Sci. 375 (2012) 154–159.
[17] R.Z. Chen, C.Y. Zhi, H. Yang, Y. Bando, Z.Y. Zhang, N. Sugiur, Arsenic (V) adsorption on Fe_3O_4 nanoparticle-coated boron nitride nanotubes, J. Colloid Interface Sci. 359 (2011) 261–268.
[18] D.S. Han, A. Abdel-Wahab, B. Batchelor, Surface complexation modeling of arsenic(III) and arsenic(V) adsorption onto nanoporous titania adsorbents (NTAs), J. Colloid Interface Sci. 348 (2010) 591–599.
[19] T.Z. Minović, J.J. Gulicovski, M.M. Stoiljković, B.M. Jokić, L.S. Živković, B.Z. Matović, B.M. Babić, Surface characterization of mesoporous carbon cryogel and its application in arsenic (III) adsorption from aqueous solutions, Microporous Mesoporous Mater. 201 (2015) 271–276.
[20] H.A. Menezes, G. Maia, Specific adsorption of arsenic and humic acid on Pt and PtO films, Electrochim. Acta 55 (2010) 4942–4951.
[21] Q.G. Chang, W. Lin, W.C. Ying, Preparation of iron-impregnated granular activated carbon for arsenic removal from drinking water, J. Hazard. Mater. 184 (2010) 515–522.

[22] R. Dobrowolski, M. Otto, Preparation and evaluation of Ni-loaded activated carbon for enrichment of arsenic for analytical and environmental purposes, Microporous Mesoporous Mater. 179 (2013) 1–9.
[23] M.L. Chen, Y.M. Lin, C.B. Gu, J.H. Wang, Arsenic sorption and speciation with branch-polyethyleneimine modified carbon nanotubes with detection by atomic fluorescence spectrometry, Talanta 104 (2013) 53–57.
[24] N. Sankararamakrishnan, A. Gupta, S.R. Vidyarthi, Enhanced arsenic removal at neutral pH using functionalized multiwalled carbon nanotubes, J. Environ. Chem. Eng. 2 (2014) 802–810.
[25] Y.S. Ho, G. McKay, A comparison of chemisorption kinetic models applied to pollutant removal on various sorbents, Process Saf. Environ. Prot. 76 (1998) 332–340.
[26] D.M. Sahabi, M. Takeda, I. Suzuki, J.I. Koizumi, Adsorption and abiotic oxidation of arsenic by aged biofilter media: Equilibrium and kinetics, J. Hazard. Mater. 168 (2009) 1310–1318.
[27] Z.M. Ren, G.S. Zhang, J.P. Chen, Adsorptive removal of arsenic from water by an iron-zirconium binary oxide adsorbent, J. Colloid Interface Sci. 358 (2011) 230–237.
[28] W. Stumm, J.J. Morgan, Aquatic Chemistry: Chemical Equilibria and Rates in Natural Water, Wiley, New York, NY, 1996.
[29] M.M. Benjamin, Water Chemistry, McGraw-Hill, New York, NY, 2002.
[30] F. Di Natale, A. Erto, A. Lancia, D. Musmarra, Experimental and modelling analysis of As(V) ions adsorption on granular activated carbon, Water Res. 42 (2008) 2007–2016.
[31] D. Mohan, C.U. Pittman Jr., Arsenic removal from water/wastewater using adsorbents—A critical review, J. Hazard. Mater. 142 (2007) 1–53.
[32] Y.M. Pajany, C. Hurel, N. Marmier, M. Roméo, Arsenic (V) adsorption from aqueous solution onto goethite, hematite, magnetite and zero-valent iron: Effects of pH, concentration and reversibility, Desalination 281 (2011) 93–99.